

Coupled spin-charge order in frustrated itinerant triangular magnets

Sahinur Reja,¹ Rajyavardhan Ray,² Jeroen van den Brink,¹ and Sanjeev Kumar²

¹*Institute for Theoretical Solid State Physics, IFW Dresden, 01171 Dresden, Germany*

²*Indian Institute of Science Education and Research (IISER) Mohali, Sector 81, S.A.S. Nagar, Manauli PO 140306, India*

(Received 1 December 2014; published 9 April 2015)

We uncover four spin-charge ordered ground states in the strong coupling limit of the Kondo lattice model on triangular geometry. The results are obtained using Monte Carlo simulations, with a classical treatment of localized moments. Two of the states at one-third electronic filling ($n = 1/3$) consist of decorated ferromagnetic chains coupled antiferromagnetically with the neighboring chains. The third magnetic ground state is noncollinear, consisting of antiferromagnetic chains separated by a pair of canted ferromagnetic chains. An even more unusual magnetic ground state, a variant of the 120° Yafet-Kittel phase, is discovered at $n = 2/3$. These magnetic orders are stabilized by opening a gap in the electronic spectrum: a “band effect.” All the phases support modulations in the electronic charge density due to the presence of magnetically inequivalent sites. In particular, the charge ordering pattern found at $n = 2/3$ is observed in various triangular lattice systems, such as $2H$ -AgNiO₂, $3R$ -AgNiO₂, and Na_xCoO₂.

DOI: [10.1103/PhysRevB.91.140403](https://doi.org/10.1103/PhysRevB.91.140403)

PACS number(s): 71.27.+a, 71.10.-w, 71.45.Lr, 75.10.-b

The influence of conduction electrons on the behavior of a system of localized magnetic moments is a well-studied topic in solid state physics. Investigations of such spin-charge coupled systems have given rise to a number of key concepts in magnetism and transport, such as the Ruderman-Kittel-Kasuya-Yosida (RKKY) interactions, the Kondo effect, and the double-exchange (DE) mechanism [1–6]. These concepts are commonly invoked in order to understand magnetism and charge transport in materials ranging from dilute magnetic semiconductors to various transition metal oxides and heavy fermion compounds [7,8]. In recent years, it has been realized that the geometry of the underlying lattice plays a crucial role in determining the nature of magnetic states in such systems [9–12]. In particular, geometrically frustrated lattices support unusual noncollinear and even noncoplanar spin textures in the ground states [11–16]. The electronic response is dramatically affected by these unusual spin textures, exhibiting remarkable phenomena such as colossal magnetoresistance, anomalous and quantum anomalous Hall effects, and multiferroicity [17–19]. As a result of such diversity of phenomena associated with unusual spin textures, their search in models, materials, and artificial structures has become a very active field of research [20–24].

The starting point for a theoretical analysis of the interplay between spin-charge coupling and magnetic frustrations is the Kondo-lattice model (KLM) on various frustrated geometries. Historically, the KLM describes localized quantum spins coupled antiferromagnetically to conduction electrons. However, it is also commonly used for systems with a ferromagnetic coupling and large local moments [11,13–15]. In the limit of weak Kondo coupling, the shape of Fermi surface can play a crucial role in determining the magnetic ground state [11,25]. Moreover, a perturbative expansion of free energy to various orders in Kondo coupling can be used to derive effective magnetic Hamiltonians [26]. However, in a strong coupling limit, the relevance of a noninteracting Fermi surface or that of a perturbative effective Hamiltonian in determining magnetic ground states is less clear. Nevertheless, there are many examples where the magnetic order in the strong coupling limit turns out to be the same as that in the weak coupling limit [11,13,15].

The focus of this Rapid Communication is the strong coupling limit of the KLM on triangular lattice. We establish the presence of four exotic spin-charge ordered ground states at filling fractions of $n = 1/3$ and $n = 2/3$. Two of these phases are collinear, and consist of decorated ferromagnetic (FM) chains. The other two phases are noncollinear (NC), of which one can be visualized as antiferromagnetic (AF) chains separated by a pair of canted-FM chains. The other NC phase is similar to the 120° state, except that it consists of three types of spin triangles. An inequivalence between the lattice sites is induced by the peculiar spin ordering, causing an ordering of the electronic charge density. While the charge modulations are weak for phases at $n = 1/3$, a strong charge ordering is found at $n = 2/3$ with an ordering pattern similar to that observed in experiments on various triangular lattice systems [27–33]. We show that two of the four phases are further stabilized by Coulomb repulsions. The existence of such spin-charge orderings in a realistic model could guide the experimental search for unusual magnetic ordering phenomena.

We start from the KLM consisting of localized moments coupled to itinerant fermions. Assuming the moments to be classical, the model in the strong coupling limit reduces to a DE model with additional AF exchange [15,34–36]. The resulting Hamiltonian on the triangular lattice is

$$H = - \sum_{\langle ij \rangle} (t_{ij} c_i^\dagger c_j + \text{H.c.}) + J_{\text{AF}} \sum_{\langle ij \rangle} \mathbf{S}_i \cdot \mathbf{S}_j, \quad (1)$$

where c_i (c_i^\dagger) is the usual annihilation (creation) operator for electron with spin parallel to the local magnetic moment \mathbf{S}_i . The angular brackets in the summations denote the nearest-neighbor (NN) pairs of sites on a triangular lattice. J_{AF} is the strength of AF coupling between NN localized spins. Note that t_{ij} depend on the polar and azimuthal angles $\{\theta_i, \phi_i, \theta_j, \phi_j\}$ of the NN core spins, and are given by $t_{ij} = t_0 [\cos(\theta_i/2) \cos(\theta_j/2) + \sin(\theta_i/2) \sin(\theta_j/2) e^{i(\phi_i - \phi_j)}]$ [34]. Previous studies show that the classical approximation is a good starting point, unless the localized moments are spin- $\frac{1}{2}$ [37,38]. The parameters of the model are the hopping

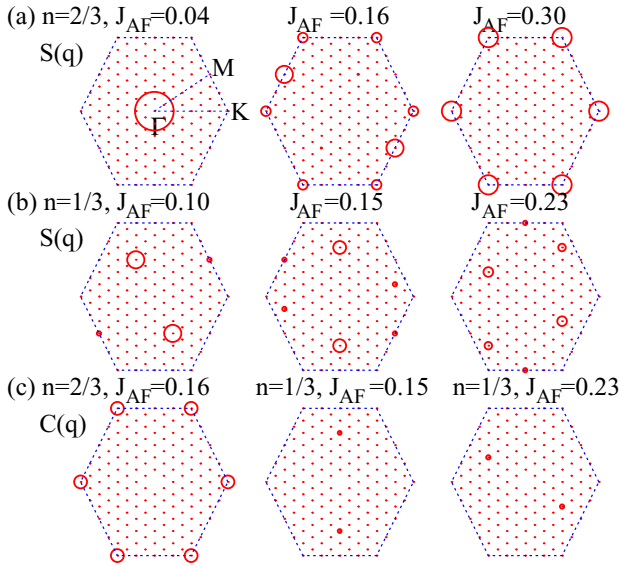


FIG. 1. (Color online) (a), (b) Low-temperature spin structure factor for different values of J_{AF} at $n = 2/3$ and $n = 1/3$. (c) Charge structure factor for three representative values of J_{AF} at $n = 2/3$ and $n = 1/3$. The circle size at a given \mathbf{q} represents the magnitude of the structure factor at that \mathbf{q} .

amplitude t_0 , the AF coupling J_{AF} , and the electronic filling fraction n . We set $t_0 = 1$ as the reference energy scale.

The model is investigated using the state of the art Monte Carlo (MC) method which combines the classical MC for spins with numerical diagonalization for fermions [39]. The solution of a fermionic problem is carried out numerically at each MC update step in order to obtain the electronic contribution to the total energy of a given classical spin configuration. We have used 6^2 and 12^2 clusters with periodic boundary conditions and typically 10^4 MC steps for equilibration and averaging. While the MC on larger lattices is not feasible due to computational costs, the energies of candidate states have been compared on 1200^2 sites [40].

The important physical quantity that contains information about the nature of magnetic ordering is the spin structure factor $[S(\mathbf{q})]$, which is defined as

$$S(\mathbf{q}) = \frac{1}{N^2} \sum_{ij} \langle \mathbf{S}_i \cdot \mathbf{S}_j \rangle_{av} e^{-i\mathbf{q} \cdot (\mathbf{r}_i - \mathbf{r}_j)}. \quad (2)$$

In the above, $\langle \dots \rangle_{av}$ denotes the thermal or MC average, N is the number of lattice sites, and $\mathbf{r}_i, \mathbf{r}_j$ are the position vectors of sites i, j . We begin by discussing the spin structure factor results obtained from simulations on a 12×12 lattice. Figures 1(a) and 1(b) display the results at low temperature, $T = 0.002t_0$, for filling fractions $n = 2/3$ and $n = 1/3$, respectively. The magnitude of $S(\mathbf{q})$ is indicated by the radius of the open circles, and the \mathbf{q} values are restricted to the first Brillouin zone. In the low- J_{AF} limit, the $S(\mathbf{q})$ peaks at the Γ point, indicating a ferromagnetic ground state, which is expected in the DE model. For $n = 1/3$, the peak at the Γ point remains robust in the range $0 \leq J_{AF} < 0.08$. For $J_{AF} = 0.10$, we find two peaks in the $S(\mathbf{q})$ [see Fig. 1(b)], one at the M point and the other on the $\Gamma - K$ axis. For $J_{AF} = 0.16$, $S(\mathbf{q})$ indicates the presence of another unusual magnetic phase with

peaks at multiple \mathbf{q} points. We confirm by looking at the spin configurations in real space that both these phases are collinear. The $S(\mathbf{q})$ at $J_{AF} = 0.23$ is qualitatively different, indicating the appearance of yet another magnetic order. We will discuss the nature of these phases in detail later. The plots at different values of J_{AF} are only representative of different phases. The stability range of these phases will become clear when we discuss the phase diagrams.

For $n = 2/3$, the presence of another unusual magnetic order in the coupling range $0.04 < J_{AF} < 0.20$ is inferred from the $S(\mathbf{q})$. This phase is characterized by two peaks in the $S(\mathbf{q})$ at the K and M points [see Fig. 1(a) plotted for $J_{AF} = 0.16$]. It is also clear from the structure factor plots that all the different phases discussed above break the threefold rotational symmetry of the triangular lattice. In order to further probe the nature of electronic states in these magnetic phases, we compute the charge structure factor, defined as

$$C(\mathbf{q}) = \frac{1}{N^2} \sum_{ij} \langle \delta n_i \delta n_j \rangle_{av} e^{-i\mathbf{q} \cdot (\mathbf{r}_i - \mathbf{r}_j)}, \quad (3)$$

where $\delta n_i = n_i - n$ is the charge density modulation with regard to the average charge density n . The $C(\mathbf{q})$ plots in Fig. 1(c) show that all the magnetic phases discussed above exhibit charge ordering. For the phases at $n = 1/3$, the magnitude of charge disproportionation is small, and the ordering pattern is striplike. However, for the NC magnetic phase at $n = 2/3$, the charge ordering is strong in magnitude, and has a pattern similar to the one observed in various triangular lattice systems with an active spin degree of freedom, such as $2H\text{-AgNiO}_2$, $3R\text{-AgNiO}_2$, and Na_xCoO_2 [27–33]. Typically, a CO state arises either due to Coulomb repulsions at appropriate filling fractions, or due to charge-lattice couplings [41]. Therefore, it is unusual that charge ordering emerges in a model consisting of local charge-spin coupling. Indeed, this was emphasized in a recent work reporting the presence of an unusual spin-charge ordered state in KLM [42].

We now discuss in detail the phase diagram of the model at $n = 1/3$. In Fig. 2(a), we plot the ground-state energy for different J_{AF} values obtained from MC simulations. Looking at the low- T spin configurations from the simulations, we infer the nature of magnetic ground states for different J_{AF} . The straight lines in Fig. 2(a) correspond to the energy obtained for ideal long-range ordered spin arrangements. For small J_{AF} , the MC energies fall on the straight line corresponding to a FM phase, as expected. Similarly, in the limit of large J_{AF} , the MC energies match well with those of the 120° Yafet-Kittel (YK) phase. We require four additional magnetic phases in order to fit the MC data in the intermediate J_{AF} regime. The spin arrangement for three of these magnetic phases are shown in Figs. 2(c)–2(e). We label two of these phases as decorated stripes (DS1 and DS2), and the third as canted AF (C-AF). The fourth phase will be discussed later, as it turns out to be the dominant phase at $n = 2/3$.

In order to visualize these phases more clearly, we have connected all the ferromagnetically oriented spins via solid lines. This highlights the main feature of DS1 [see Fig. 2(c)], that this phase consists of diamond-shaped FM chains running along one direction connected antiferromagnetically to the neighboring spins. Similarly, the DS2 phase consists of FM

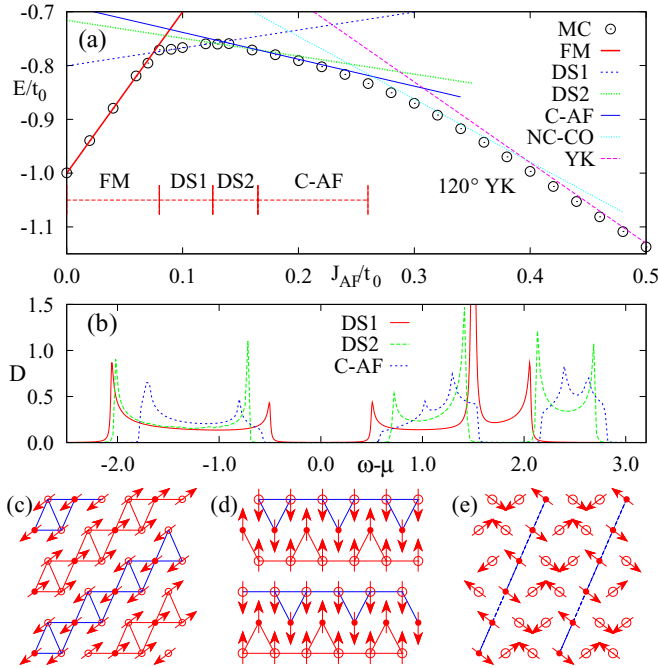


FIG. 2. (Color online) (a) Energy per site at $T/t_0 = 0.002$ as a function of J_{AF} obtained via MC simulations (circles) for a filling fraction of $n = 1/3$. Various straight lines are the energies of different phases as indicated by legends. (b) The electronic density of states for three ground states, DS1, DS2, and C-AF. (c)–(e) Snapshots of the MC configurations for the three ground states. The arrows indicate the spin directions, and the circle sizes indicate the local charge density. The smaller circles have been filled to highlight the pattern of charge ordering.

stripes decorated by triangular units [see Fig. 2(d)]. In the strong Kondo coupling limit, the electronic hopping across a pair of sites hosting antiferromagnetically oriented spins is zero. Therefore, in the DS1 and DS2 phases, the electronic problem becomes one dimensional. The electronic density of states (DOS) in the decorated stripe phases has large gaps at the chemical potential [see Fig. 2(b)]. The opening of these gaps in the DOS lowers the total energy of the system and hence these unusual phases are stabilized. Such decorated stripe paths for hopping are realized in certain organic polymers [43,44], and are also of interest to researchers working on exactly solvable models of electronic correlations [45,46]. Interestingly, such structures for fermion hopping can emerge in a higher dimensional lattice via a subtle interplay between geometrical frustrations and spin-charge coupling.

The two phases discussed so far are collinear in nature and therefore allow for a description in terms of FM chains. The third phase at $n = 1/3$ is NC, and consists of AF chains separated by a pair of canted FM chains. This spin arrangement also opens a gap in the electronic DOS at the chemical potential. All the phases discussed above contain inequivalent sites in terms of the orientation of neighboring spins. This causes a modulation in the local charge density, and indeed we find a charge ordering in all the phases [see Figs. 2(c)–2(e)]. For opening a gap in the spectrum, which we find in all the three phases discussed above, the entire magnetic structure must be modified. This can be seen as a “band effect.” It is

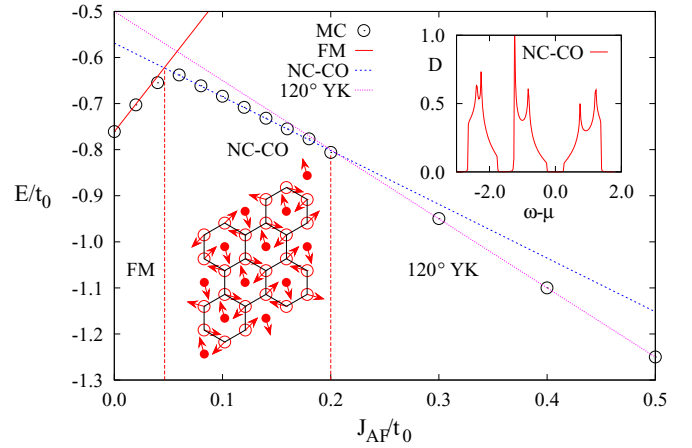


FIG. 3. (Color online) Ground-state energy per site as a function of J_{AF} obtained via MC simulations (circles) for a filling fraction of $n = 2/3$. The solid, dashed, and dotted straight lines are the energies of ferromagnetic, NC-CO, and the 120° Yafet-Kittel states, respectively. The lower inset shows the snapshot of the MC ground state with the arrows representing the spin directions and the circle sizes indicating the local charge density. The smaller circles have been filled and high charge density points are connected by lines to highlight the real-space pattern of charge ordering. The inset in the top-right corner shows the density of states for the NC-CO state.

also interesting to note that the DS1 and DS2 spontaneously break a discrete rotational symmetry. Since there cannot be any magnetic order at finite temperatures in a rotationally invariant continuous spin model [47], it may give rise to an interesting nematic magnetic order at finite temperatures. These magnetic phases exist in the wide parameter range $0.08 < J_{AF} < 0.26$. For larger values of J_{AF} the magnetic order gradually changes towards the 120° YK phase. We note that in the range $0.26 < J_{AF} < 0.36$ the energy of another unusual spin-charge ordered state is close to that obtained from MC simulations. In fact, the same state dominates the phase diagram at $n = 2/3$, which we discuss next.

In Fig. 3, we show the low- T MC energy for different values of J_{AF} at $n = 2/3$. Following the analysis at $n = 1/3$, we compare the MC energies with those obtained for ideal ordered spin patterns. We require only three phases to perfectly describe the MC energy data across the full J_{AF} range. Two of these phases are the expected limiting phases: a ferromagnet at small values of J_{AF} and a 120° YK phase at large J_{AF} . The entire intermediate range belongs to another exotic spin-charge ordered phase. A MC snapshot of this magnetic phase at low temperature is shown in the inset in Fig. 3. The spin structure remains planar, as in the 120° phase. In fact, for a specific choice of global orientation, all spins are pointing towards the neighboring sites, which is also similar to the 120° phase. The important difference is that in this phase, there are three different types of triangles, as shown in the real-space plot in Fig. 3. The first type is the usual 120° orientation, the second type is formed with two antiparallel spins, with the third one pointing at 60° . The third type of triangle can be obtained from the second type by flipping the spins. Similar to other magnetic phases discussed so far, this magnetic arrangement also generates inequivalent sites

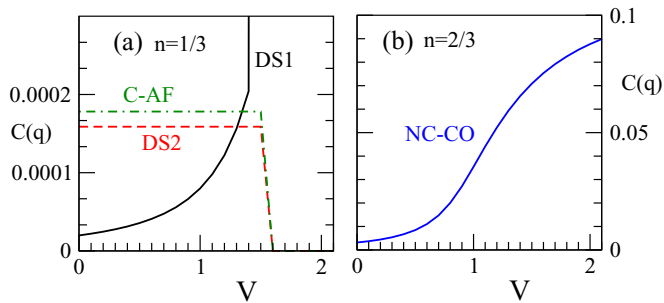


FIG. 4. (Color online) The change in the peak intensity of the charge structure factors at characteristic \mathbf{q} for the four different spin-charge ordered phases at (a) $n = 1/3$ and (b) $n = 2/3$, with increasing NN Coulomb repulsion V .

in terms of the hopping amplitudes. This inequivalence is reflected via a charge ordering pattern (see the inset in Fig. 3) that closely resembles the charge modulations observed in various triangular lattice materials [27–30]. In particular, a state with *six* magnetically inequivalent Co ions has recently been observed in NMR experiments on Na_xCoO_2 [31,32]. The electronic DOS in this magnetic phase supports two gaps (see the inset in Fig. 3), corresponding to filling fractions of $n = 2/3$, and $n = 1/3$, thereby justifying the existence of the NC-CO phase at both filling fractions.

In order to test the stability of these unusual spin-charge ordered phases in the presence of electron-electron interactions, we add to the Hamiltonian Eq. (1) a NN repulsive interaction, $H_I = V \sum_{\langle ij \rangle} n_i n_j$. An unrestricted Hartree-Fock analysis is performed by keeping the magnetic order fixed [40]. The $C(\mathbf{q})$ is then computed for the self-consistent solutions for local charge densities. We plot in Fig. 4 the magnitude of the $C(\mathbf{q})$ at characteristic values of q as a function of V for each of the four ordered phases. Two of the phases at $n = 1/3$, DS2 and

C-AF, are not affected by the NN repulsive interaction [see Fig. 4(a)]. However, beyond a critical value of V , these phases are destabilized in favor of the expected charge ordered phase consisting of a high density site surrounded by low density sites. On the contrary, the structure factors for DS1 and NC-CO states increase with increasing V , indicating that both these states are further stabilized by a NN repulsive interaction.

To conclude, we have reported four spin-charge ordered phases at filling fractions of $n = 1/3$ and $n = 2/3$ in the strong coupling KLM on a triangular lattice. Two of these phases are collinear and stripelike in their magnetic arrangement, and the other two are noncollinear. The presence of magnetically inequivalent sites leads to charge ordering in all the phases. The charge ordering pattern for the noncollinear phase at $n = 2/3$ is identical to that observed in various triangular lattice materials with an active spin degree of freedom, such as $2H\text{-AgNiO}_2$, $3R\text{-AgNiO}_2$, and Na_xCoO_2 [27–33]. The inclusion of a NN Coulomb interaction enhances the charge ordering further, indicating that mutually supportive mechanisms could be involved in stabilizing such ordering in real materials. The stability of these states relies on the nature of the electronic spectrum for itinerant fermions, which develops a gap at the chemical potential. Consequently, all the phases reported in this study are electrically insulating with a gap of the order of the bare hopping amplitude. These insulators can neither be called Slater type nor Mott type since the opening of the gap can neither be understood from the Fermi surface nesting arguments nor from the infinite coupling limit. Therefore, such exotic spin-charge ordered insulators are prototype examples of cooperative many-body effects which are not easy to understand within effective single particle theories.

We thank Maria Daghofer for useful discussions. S.K. acknowledges the hospitality at IFW Dresden during June–July 2014, and financial support from the Department of Science and Technology, India.

-
- [1] M. A. Ruderman and C. Kittel, *Phys. Rev.* **96**, 99 (1954).
 [2] T. Kasuya, *Prog. Theor. Phys.* **16**, 45 (1956).
 [3] K. Yosida, *Phys. Rev.* **106**, 893 (1957).
 [4] J. Kondo, *Prog. Theor. Phys.* **32**, 37 (1964).
 [5] C. Zener, *Phys. Rev.* **82**, 403 (1951).
 [6] P. G. de Gennes, *Phys. Rev.* **118**, 141 (1960).
 [7] T. Dietl and H. Ohno, *Rev. Mod. Phys.* **86**, 187 (2014).
 [8] G. Stewart, *Rev. Mod. Phys.* **56**, 755 (1984).
 [9] H. Ishizuka and Y. Motome, *Phys. Rev. Lett.* **109**, 237207 (2012).
 [10] H. Ishizuka and Y. Motome, *Phys. Rev. B* **87**, 155156 (2013).
 [11] I. Martin and C. D. Batista, *Phys. Rev. Lett.* **101**, 156402 (2008).
 [12] G.-W. Chern, *Phys. Rev. Lett.* **105**, 226403 (2010).
 [13] Y. Akagi and Y. Motome, *J. Phys. Soc. Jpn.* **79**, 083711 (2010).
 [14] Y. Motome and N. Furukawa, *Phys. Rev. Lett.* **104**, 106407 (2010).
 [15] S. Kumar and J. van den Brink, *Phys. Rev. Lett.* **105**, 216405 (2010).
 [16] J. W. F. Venderbos, M. Daghofer, J. van den Brink, and S. Kumar, *Phys. Rev. Lett.* **109**, 166405 (2012).
 [17] M. Salamon and M. Jaime, *Rev. Mod. Phys.* **73**, 583 (2001).
 [18] N. Nagaosa, J. Sinova, S. Onoda, A. H. MacDonald, and N. P. Ong, *Rev. Mod. Phys.* **82**, 1539 (2010).
 [19] S.-W. Cheong and M. Mostovoy, *Nat. Mater.* **6**, 13 (2007).
 [20] S. Banerjee, O. Erten, and M. Randeria, *Nat. Phys.* **9**, 626 (2013).
 [21] J. Wang, B. Lian, and S.-C. Zhang, *arXiv:1409.6715*.
 [22] T. Liu, B. Douçot, and K. L. Hur, *arXiv:1409.6237*.
 [23] R. F. Wang, C. Nisoli, R. S. Freitas, J. Li, W. McConville, B. J. Cooley, M. S. Lund, N. Samarth, C. Leighton, V. H. Crespi, and P. Schiffer, *Nature (London)* **439**, 303 (2006).
 [24] C. Nisoli, R. Moessner, and P. Schiffer, *Rev. Mod. Phys.* **85**, 1473 (2013).
 [25] S. Hayami and Y. Motome, *Phys. Rev. B* **90**, 060402 (2014).
 [26] Y. Akagi, M. Udagawa, and Y. Motome, *Phys. Rev. Lett.* **108**, 096401 (2012).

- [27] E. Wawrzyńska, R. Coldea, E. M. Wheeler, T. Sörgel, M. Jansen, R. M. Ibberson, P. G. Radaelli, and M. M. Koza, *Phys. Rev. B* **77**, 094439 (2008).
- [28] E. Wawrzyńska, R. Coldea, E. M. Wheeler, I. I. Mazin, M. D. Johannes, T. Sörgel, M. Jansen, R. M. Ibberson, and P. G. Radaelli, *Phys. Rev. Lett.* **99**, 157204 (2007).
- [29] C. Bernhard, A. V. Boris, N. N. Kovaleva, G. Khaliullin, A. V. Pimenov, L. Yu, D. P. Chen, C. T. Lin, and B. Keimer, *Phys. Rev. Lett.* **93**, 167003 (2004).
- [30] J.-H. Chung, J.-H. Lim, Y. J. Shin, J.-S. Kang, D. Jaiswal-Nagar, and K. H. Kim, *Phys. Rev. B* **78**, 214417 (2008).
- [31] I. R. Mukhamedshin, H. Alloul, G. Collin, and N. Blanchard, *Phys. Rev. Lett.* **93**, 167601 (2004).
- [32] I. R. Mukhamedshin, I. F. Gilmudinov, M. A. Salosin, and H. Alloul, *JETP Lett.* **99**, 471 (2014).
- [33] I. Mukhamedshin and H. Alloul, *Physica B* **460**, 58 (2015).
- [34] E. Müller-Hartmann and E. Dagotto, *Phys. Rev. B* **54**, R6819 (1996).
- [35] E. Dagotto, T. Hotta, and A. Moreo, *Phys. Rep.* **344**, 1 (2001).
- [36] E. Dagotto, *Nanoscale Phase Separation and Colossal Magnetoresistance* (Springer, Berlin, 2002).
- [37] E. Dagotto, S. Yunoki, A. L. Malvezzi, A. Moreo, J. Hu, S. Capponi, D. Poilblanc, and N. Furukawa, *Phys. Rev. B* **58**, 6414 (1998).
- [38] J. Kienert and W. Nolting, *Phys. Rev. B* **73**, 224405 (2006).
- [39] S. Yunoki, J. Hu, A. L. Malvezzi, A. Moreo, N. Furukawa, and E. Dagotto, *Phys. Rev. Lett.* **80**, 845 (1998).
- [40] See Supplemental Material at <http://link.aps.org/supplemental/10.1103/PhysRevB.91.140403> for further details.
- [41] S. Kumar and J. van den Brink, *Phys. Rev. B* **78**, 155123 (2008).
- [42] T. Misawa, J. Yoshitake, and Y. Motome, *Phys. Rev. Lett.* **110**, 246401 (2013).
- [43] J.-W. van der Horst, P. A. Bobbert, M. A. J. Michels, G. Brocks, and P. J. Kelly, *Phys. Rev. Lett.* **83**, 4413 (1999).
- [44] M. Côté, P. D. Haynes, and C. Molteni, *Phys. Rev. B* **63**, 125207 (2001).
- [45] Z. Gulácsi, A. Kampf, and D. Vollhardt, *Phys. Rev. Lett.* **99**, 026404 (2007).
- [46] Z. Gulácsi, A. Kampf, and D. Vollhardt, *Phys. Rev. Lett.* **105**, 266403 (2010).
- [47] D. Loss, F. L. Pedrocchi, and A. J. Leggett, *Phys. Rev. Lett.* **107**, 107201 (2011).